

Real-time elastography for detecting prostate cancer: preliminary experience

Leo Pallwein, Michael Mitterberger*, Peter Struve, Germar Pinggera*, Wolfgang Horninger*, Georg Bartsch*, Friedrich Aigner, Andreas Lorenzt, Florian Pedross† and Ferdinand Frauscher

Departments of Radiology II, *Urology, †Medical Statistics, Information and Health Economics, Medical University Innsbruck, Austria, and †LP-IT Innovative Technologies GmbH, Bochum, Germany

Accepted for publication 12 January 2007

OBJECTIVE

To assess the use of real-time elastography (RTE) for detecting prostate cancer in patients scheduled for radical prostatectomy (RP), as most solid tumours differ in their consistency from the deriving tissue, and RTE might offer a new tool for cancer detection.

PATIENTS AND METHODS

We examined 15 patients (mean age 56 years, SD 6.2, range 46–71) with RTE, using an ultrasonography (US) system with a 7.5-MHz transrectal probe as a transducer. RTE is capable of visualizing displacements between pairs of US images of tissues when placed under axial compression. The stiffness of the lesion was displayed from blue (soft) to black (hard). Hard lesions with a diameter of ≥ 5 mm were considered as malignant. All patients had the diagnosis of prostate cancer

confirmed by biopsy and had a mean (range) prostate specific antigen (PSA) level of 4.6 (1.4–16.1) ng/mL; all were scheduled for RP. US was performed by two investigators and interpreted by consensus. Cancer location and size was determined in the RTE mode only. One pathologist classified tumour location, grade and stage. The RTE findings were compared with the pathological findings.

RESULTS

There were no major complications during RP in any patient; all had a pT2 tumour on histopathological examination, the Gleason score was 5–9 and the mean (range) tumour size 1.1 (0.6–2.5) cm. Thirty-five foci of prostate cancer were present at the pathological evaluation; multiple foci were found in 11 of the 15 glands. RTE detected 28 of 35 cancer foci (sensitivity 80%). The per-

patient analysis showed that RTE detected at least one cancer area in each of the 15 patients. Only four sites with false-positive findings on RTE and no histopathological correlation were detected; these findings were obtained in the first five patients (period of learning).

CONCLUSIONS

RTE can be used to visualize differences in tissue elasticity. Our results show that RTE allows the detection of prostate cancer and estimation of tumour location and size. RTE of the prostate is a new imaging method with great potential for detecting prostate cancer.

KEYWORDS

ultrasonography, prostate cancer, elastography, detection

INTRODUCTION

Prostate cancer is the most common cancer in men, and with an increasingly ageing population at greater risk of prostate cancer, it is expected that this will result in a further increase in the incidence in the next few years [1]. The diagnosis of prostate cancer is based on PSA testing, the DRE and ultrasonography (US)-guided biopsy. Systematic biopsy with at least 8–10 cores is the method of choice. Prostate cancer imaging is the focus of intense research effort, and cancer detection has improved in the last decade, mainly through contrast-enhanced TRUS and functional and structural endorectal MRI studies [2–7]. The results of MRI are promising, but this method remains expensive and not always available. The detection rate of

a malignant lesion in the prostate with these techniques is 15–60%, mainly depending on the PSA value and stage of disease. However, early detection is the key to successful treatment.

Single grey-scale US has several limitations for detecting prostate cancer; one is that the chance a hypoechoic area containing cancer is 17–57%, which leads to a low sensitivity and specificity [2]. Another limitation is that even taking more biopsy cores and more laterally directed biopsies, the prostate cancer detection rate cannot be increased even with 24 cores [8]. Therefore, new techniques for cancer detection seem to be desirable.

Krouskop *et al.* [9] reported that cell density was greater in neoplastic tissue, which causes

a change in tissue elasticity/stiffness. Elastography (strain imaging) is a new technique, which allows an assessment of tissue elasticity; Ophir *et al.* [10] first described the principle of this technique in 1991. To reduce the time-consuming calculations, Pesavento *et al.* [11] developed a fast cross-correlation technique that is the basis for real-time elastography (RTE). This imaging method can be used to visualize displacements between US image-pairs of tissue under 'compression' [10–13]. As most solid tumours differ in their consistency from the deriving tissue, RTE offers a novel tool for detecting cancer. Thus, the goal of the present preliminary study was to assess the value of RTE for detecting prostate cancer in patients scheduled for radical prostatectomy (RP).

FIG. 1.
Explanation of RTE in a jelly phantom experiment: RTE (left image) allows the detection of a hard inclusion in this jelly phantom, which is not detectable with conventional B-mode US (right image). The stiffness of the lesion is displayed from blue (soft) to red and yellow (intermediate) and to black (hard). (Reprinted with permission [Ultraschall Med 2000; 21: 8–15].)

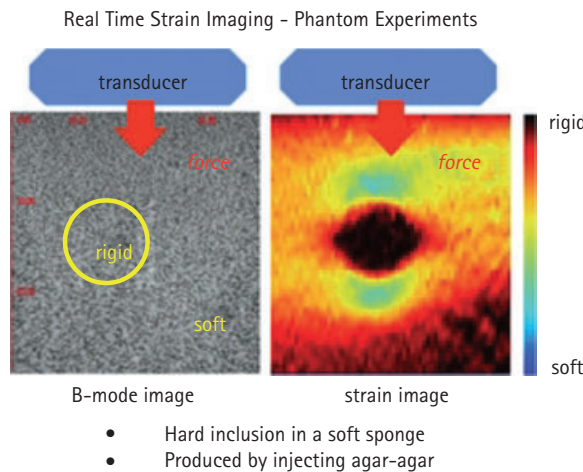
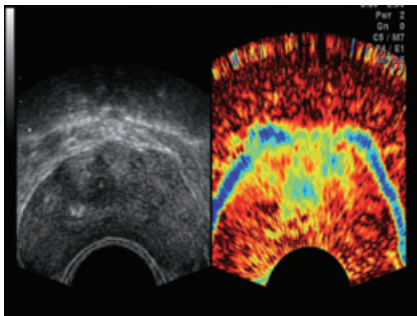


FIG. 2. B-mode image and elastogram of a normal prostate (mid-gland) with the prostate capsule delineated in blue (the so-called 'soft-rim artefact'). Note the artefacts delineating the urethra, and the reticular pattern of red and black strains in the inner and outer gland, a typical appearance of normal prostate tissue.



PATIENTS AND METHODS

Between February 2004 and July 2004 we examined 15 consecutive patients (mean age 56 years, SD 6.2, range 46–71) using RTE. We included only patients with clinically organ-confined prostate cancer confirmed by biopsy, with a mean (range) PSA level of 4.6 (1.4–16.1) ng/mL; all patients were scheduled for RP. Before RP all patients had TRUS using the conventional B-mode technique, and RTE, the latter performed by two radiologists (7–9 years of experience). The images were interpreted on-line by the two radiologists, by consensus. They were unaware of the biopsy results, clinical data and PSA values, and other US investigations. The US system used was the Voluson 730 (GE Healthcare, Chalfont St Giles, UK) with an endorectal side-fire 7.5-MHz transducer.

Tissue elasticity (strain image, elastogram) can be mapped by acquiring multiple image pairs. Compressing and releasing of the tissue with the hand-held US transducer itself induced the strain. The strain was calculated between pairs of images before and after compression using the cross-autocorrelation method, in which the echofrequency pattern of one US beam (radiofrequency data set: unfiltered, high-frequency US data) is compared over time to calculate the correlation coefficient of the echo-signals before and after compression. The limitation of this method is that the accuracy of this estimate depends on the sample time and length of acquisition [14].

The displacement estimates are used to determine the tissue strain and to reconstruct Young's modulus (estimate of time shifts between corresponding A-lines) [15–17]. Real-time evaluation was made possible by reducing the time-consuming calculation of estimates of axial displacements between radiofrequency data sets of two corresponding US images, using a new phase-root-seeking technique [11]. The strain imaging views were calculated using a frame rate of up to 30 frames/s. Within a region of interest of $\approx 2.5 \times 3.6$ cm the real-time strain images were calculated and displayed.

Multi-compression imaging was used, i.e. the examiner repeated the procedure of compression and decompression to improve the signal-to-noise ratio of the strain images to obtain reliable elastograms from the region of interest [18]. The absolute value of the strain was displayed as colour-encoded at the US monitor, next to the B-mode image (Fig. 1). The stiffness of the lesion was displayed from

blue (soft), to red and yellow (intermediate), to black (hard).

Each prostate was divided into six outer gland areas (base, mid-plane, apex) [19], and each of these areas was evaluated for the existence and size of stiffer foci in the elastography mode (Fig. 2). The inner gland findings from RTE were not included in the results, based on two considerations: (i) in a PSA screening population we found that transition zone (TZ) cancers are very rare [20]; (ii) RTE can produce 'stiffness' artefacts with increasing depth of US penetration. The diagnosis of prostate cancer was based only on the RTE criteria, as described by Konig *et al.* [12]: (i) hard lesions were considered as suspicious for prostate cancer; (ii) only hard lesions with a diameter of ≥ 5 mm were included; (iii) the strain image of the lesion was reproducible (after tilting the US probe).

Only lesions that fulfilled all criteria were considered to be malignant. The simultaneously displayed B-mode images served only for topographic orientation and not for tumour detection.

After RP, one pathologist classified tumour location, grade and stage; the RTE findings were then compared with the histopathological findings. For a better comparison, only tumours with a diameter of ≥ 5 mm were included. After finishing the analysis, the pathologist assigned each tumour to an outer or inner gland area, according to the topographical system above [19].

The patients' characteristics were summarized with frequencies and percentages or as the mean (SD) and range. The sensitivity for RTE was calculated by comparison with the histopathological findings after RP (the reference standard). To calculate the correlation between RTE and Gleason score we used the contingency coefficient. A normal distribution of PSA values was assessed using the Kolmogorov–Smirnov test. Also, the 95% CI were calculated for some characteristics. All reported *P* values were two-sided and an error level of 5% was used.

RESULTS

All 15 patients had RP with no major complications during or immediately afterward; patients left the hospital at

Site	Number of cancer foci	Number and sensitivity of hard lesions	TABLE 1 The site and numbers of pathological and RTE findings
Apex right	9	9	
Mid-gland right	6	6	
Base right	2	1	
Apex left	4	4	
Mid-gland left	8	7	
Base left	3	1	
Inner gland right	2	NA	
Inner gland left	1	NA	
Total, n (%)	35	28 (80)	NA, not available.

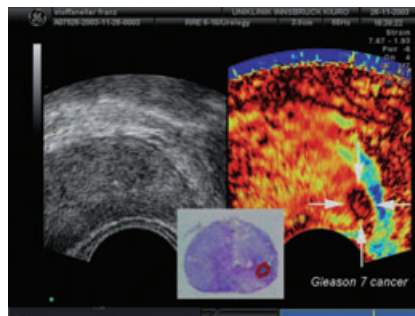
TABLE 2 The sensitivity, specificity, positive and negative predictive values, and the accuracy of RTE, for combined inner and outer gland areas (120) and for the outer gland areas (90) alone

	Combined	Outer gland
Sensitivity	0.87	0.88
Specificity	0.92	0.93
Positive predictive value	0.80	0.88
Negative predictive value	0.95	0.93
Accuracy	0.92	0.91

7–14 days after RP. All patients had a pT2 tumour on histopathological examination, and the Gleason score was 5–9. There were multiple foci of cancer in 11 of the 15 glands. The analysis of each patient showed that RTE detected at least one cancer focus in each of the 15 patients. The mean (SD, median, range) tumour size estimated on RTE was 1.1 (0.5, 1.0, 0.6–2.5) cm. Thirty-five foci of prostate cancer were present at the pathological evaluation, 32 in the different outer gland areas and three in the inner gland (Table 1).

RTE detected 28 of 35 cancer foci (sensitivity 80%; Figs 3–5). Seven foci could not be detected with RTE, three of them in the inner gland. Of the four false-negative foci in the outer gland, three were found in the basal areas. The sensitivity, specificity, negative and positive predictive values, and the overall accuracy, are listed in Table 2. The best sensitivity for elastography was at the apex (100%) and mid-gland (94%). At the base, we could visualize only two of five foci, giving a poor sensitivity. Interestingly, the accuracy of RTE of the entire organ (inner and outer gland; 0.92) was similar to that of the outer gland alone (0.91). There were four sites with false-positive findings on RTE, with histopathological correlation; these were obtained in the first five patients, while gaining experience with the technique. The

FIG. 3. Unsuspectious B-mode image (only for topographical orientation) together with an elastogram, showing a clearly visible focal stiffer area on the left side (mid-gland) fulfilling all the criteria for a suspicious lesion and presenting a cancer area. The corresponding histopathological slice confirms a Gleason 7 prostate cancer. The changes in elasticity in the inner gland and at the contralateral side do not fulfil all criteria for a suspicious lesion.



correlation between PSA levels, Gleason scores and RTE was not significant ($P > 0.05$).

DISCUSSION

Cancer tissue shows an increase in vessel density and cell density; the increase of cell density in tumours leads to a change in tissue

FIG. 4. Unsuspectious B-mode image (only for topographical orientation) together with an elastogram showing a clearly visible focal stiffer area on the left side (base) fulfilling all the criteria for a suspicious lesion, and showing a Gleason 7 prostate cancer. Note the focal stiffer area at the contralateral side, of <5 mm and therefore not fulfilling all the criteria for a suspicious lesion.

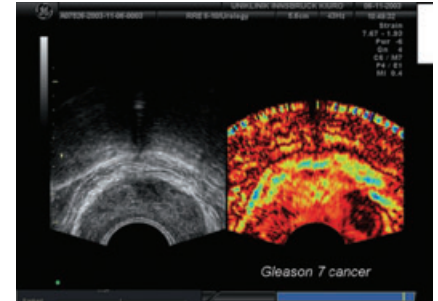
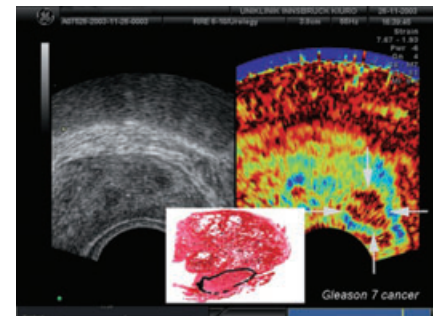


FIG. 5. Unsuspectious B-mode image (only for topographical orientation) together with an elastogram showing a clearly visible focal stiffer area on the left side (base), fulfilling all the criteria for a suspicious lesion and with a Gleason 7 prostate cancer. This lesion is surrounded by the so-called halo sign (an artificial soft rim). The changes in elasticity in the inner gland and the contralateral side do not fulfil all the criteria for a suspicious lesion.



elasticity, and Krouskop *et al.* [9] reported that there is a significant difference in stiffness between normal and neoplastic prostate and breast tissue. For detecting changes in tissue elasticity, Ophir *et al.* [10] developed an imaging technique based on static deformation, terming it 'strain imaging' or elastography.

RTE has already shown promise for detecting and differentiating masses in the breast and thyroid gland [21,22]. Cochlin *et al.* [23] introduced RTE for detecting prostate cancer in biopsy specimens. They used a different

algorithm for calculating the elastograms, based on the analysis of phase shift; for this method, the shift of Doppler frequency is calculated for the US echo signals before and after compression. The limitation of this method is the 'aliasing'. The software we used is integrated in a standard US unit and uses the cross-autocorrelation method; therefore 'aliasing' had no role. Cochlin *et al.* [23] reported that RTE had a sensitivity of 51% and a specificity of 83% for detecting prostate cancer in individual patients, and a sensitivity of 31% and specificity of 82% for detecting individually biopsied areas of the prostate.

In 2003, Sperandeo *et al.* [24] reported the usefulness of elasticity imaging to differentiate malignant from benign lesions. They used tissue elasticity to detect prostate cancer, based on tissue deformation of grey-scale images under manual compression of the prostate with a transrectal probe. In 2005, König *et al.* [12] also reported the efficacy of targeted prostate biopsy using RTE; they could enhance prostate cancer detection up to 84%.

In the present study of 15 men with clinically organ-confined prostate cancer, we used TRUS and RTE before RP to determine tumour location and size; the histopathological findings and RTE were then compared. The pathology after RP showed that all tumours were strictly organ-confined. RTE was easy in all patients, and on RTE 28 of 35 tumour foci in all patients were correctly detected for tumour size and location. RTE gave an overall sensitivity of 87% and a specificity of 92%. The best sensitivity was for detecting prostate cancer at the apex (100%) and mid-gland (94%). At the base we could visualize only two of five foci. There were only four sites with false-positive findings on RTE and no histopathological correlation, obtained in the first five patients, possibly related to gaining experience. It takes ≈ 3 months to learn the technique, because the experienced examiner can confirm the reproducibility of stiffer areas using multi-compression imaging, and after tilting the US probe.

The simultaneously displayed B-mode TRUS image can cause some biasing if there are hypoechoic lesions. However, about half the prostate cancer lesions are invisible by TRUS (i.e. isoechoic). Furthermore, two common forms of prostate pathology (prostatitis and BPH) can mimic the TRUS appearance of prostate cancer [25]. Also, in a PSA screening

population, hypoechoic areas are less common [20] and thus we did not focus on hypoechoic areas. However, in different populations it could be interesting to evaluate hypoechoic lesions on TRUS in comparison with RTE.

RTE can be used to illustrate tissue elasticity adequately to a depth of ≈ 5 cm, but we think that for BPH, and in the lateral part of the elastograms, and with increasing depth of US, many 'stiffness artefacts' are detectable. Tilting the US probe should be helpful in overcoming these 'lateral stiffness artefacts', but the 'deep stiffness artefacts' with increasing depth of US, remain a major limitation to this promising method. Therefore, RTE might not detect TZ cancers. However, in the PSA screening population, we have found that TZ cancers are very rare; in 395 cancers we found only one TZ-confined cancer (0.6%) [20]. Therefore, we think that it is reasonable to focus on the peripheral zone only in our PSA screening population. However, in other populations it would be interesting to investigate the inner gland. Accordingly, three of four false-negative findings in the present study were in the basal areas of the outer gland, giving a poor sensitivity at the base of the prostate. This might represent a limitation of this method, especially in patients with BPH.

Another main limitation of RTE is the increase in stiffness with changes in chronic inflammatory tissue, with consecutive stromal hyperplasia and fibrosis. However, different stiffness patterns were described for the thyroid gland and this detail might also be helpful in the future for the prostate [21].

Thus we list the following limitations of RTE for detecting cancer areas: (i) small tumours, although further technical development of RTE might allow an accurate detection of focal stiffer areas of < 5 mm; (ii) an increase in stiffness in chronic inflammatory tissue, i.e. prostate calcifications. (iii) BPH; (iv) no objective assessment of elasticity (i.e. strain ratio). There are some artefacts in the elastogram; some of these are of value, e.g. the 'soft rim artefact' surrounding the prostate, which might be helpful in cases of extracapsular extension. Other artefacts like the 'halo-sign' [12] were not depicted in most cases of cancer and seem to be questionable.

There are also limitations of the study protocol, the first of which was the relatively

few patients in the study. Also, two radiologists interpreted the RTE findings by consensus; therefore we have no data on inter- and intraobserver variability. The RTE findings were evaluated for the presence of cancer only, and therefore we have no data on RTE findings in BPH or other benign diseases. This might cause some bias in our study. Further studies using an RTE-based targeted approach for prostate biopsy could help to give more information about the capacity of this promising method.

In conclusion, these preliminary data show that RTE allows the detection of prostate cancer and estimates tumour location and size. Therefore, RTE of the prostate seems to be a promising imaging method with great potential for detecting prostate cancer, although further studies are needed to confirm our results.

CONFLICT OF INTEREST

There was no financial support of this study. The elastography soft- and hardware used was a work-in-progress software, and therefore supplied by the company (LP-IT, Bochum). However the US unit was owned by our department.

REFERENCES

- 1 Chodak G. Prostate cancer: epidemiology, screening, and biomarkers. *Rev Urol* 2006; **8** (Suppl. 2): S3–8
- 2 Frauscher F, Klauser A, Berger AP *et al.* [The value of ultrasound (US) in the diagnosis of prostate cancer]. *Radiologe* 2003; **43**: 455–63
- 3 Frauscher F, Klauser A, Halpern EJ, Horninger W, Bartsch G. Detection of prostate cancer with a microbubble ultrasound contrast agent. *Lancet* 2001; **357**: 1849–50
- 4 Halpern EJ, Frauscher F, Rosenberg M, Gomella LG. Directed biopsy during contrast-enhanced sonography of the prostate. *AJR Am J Roentgenol* 2002; **178**: 915–9
- 5 Dhingsa R, Qayyum A, Coakley FV *et al.* Prostate cancer localization with endorectal MR imaging and MR spectroscopic imaging: effect of clinical data on reader accuracy. *Radiology* 2004; **230**: 215–20
- 6 Cornud F, Hamida K, Flam T *et al.*

- Endorectal color doppler sonography and endorectal MR imaging features of nonpalpable prostate cancer: correlation with radical prostatectomy findings. *AJR Am J Roentgenol* 2000; **175**: 1161–8
- 7 **Beyersdorff D, Winkel A, Hamm B, Lenk S, Loening SA, Taupitz M.** MR imaging-guided prostate biopsy with a closed MR unit at 1.5 T: initial results. *Radiology* 2005; **234**: 576–81
 - 8 **Jones JS, Patel A, Schoenfield L, Rabets JC, Zippe CD, Magi-Galluzzi C.** Saturation technique does not improve cancer detection as an initial prostate biopsy strategy. *J Urol* 2006; **175**: 485–8
 - 9 **Krouskop TA, Wheeler TM, Kallel F, Garra BS, Hall T.** Elastic moduli of breast and prostate tissues under compression. *Ultrason Imaging* 1998; **20**: 260–74
 - 10 **Ophir J, Cespedes I, Ponnekanti H, Yazdi Y, Li X.** Elastography: a quantitative method for imaging the elasticity of biological tissues. *Ultrason Imaging* 1991; **13**: 111–34
 - 11 **Pesavento A, Krueger C, Ermert H.** A time efficient and accurate strain estimation concept for ultrasonic elastography using interactive phase zero estimation. *IEEE Trans an Ultrason Ferroelect Freq Contr* 1999; **46**: 1057–67
 - 12 **Konig K, Scheipers U, Pesavento A, Lorenz A, Ermert H, Senge T.** Initial experiences with real-time elastography guided biopsies of the prostate. *J Urol* 2005; **174**: 115–7
 - 13 **Ermert H.** The Ruhr Center of Competence for Medical Engineering (Kompetenzzentrum Medizintechnik Ruhr KMR, Bochum). *Biomed Tech (Berl)* 2002; **47** (Suppl. 1): 886–9
 - 14 **Frey H.** [Realtime elastography. A new ultrasound procedure for the reconstruction of tissue elasticity]. *Radiologe* 2003; **43**: 850–5
 - 15 **Skovoroda AR, Agliamov SR.** [Reconstruction of elastic properties of soft biological tissues exposed to low frequency disruption]. *Biofizika* 1995; **40**: 1329–34
 - 16 **Skovoroda AE, O'Donnell SY, M.** Tissue elasticity reconstruction based an ultrasonic displacement and strain images. *IEEE Trans an Ultrason Ferroelect Freq Contr* 1995; **42**: 747–65
 - 17 **Konofagou EE, Ophir J, Kallel F, Varghese T.** Elastographic dynamic range expansion using variable applied strains. *Ultrason Imaging* 1997; **19**: 145–66
 - 18 **Cespedes I, Ophir J.** Reduction of image noise in elastography. *Ultrason Imaging* 1993; **15**: 89–102
 - 19 **Halpern EJ, McCue PA, Aksnes AK, Hagen EK, Frauscher F, Gomella LG.** Contrast-enhanced US of the prostate with Sonazoid: comparison with whole-mount prostatectomy specimens in 12 patients. *Radiology* 2002; **222**: 361–6
 - 20 **Pelzer AE, Bektic J, Berger AP et al.** Are transition zone biopsies still necessary to improve prostate cancer detection? Results from the Tyrol screening project. *Eur Urol* 2005; **48**: 916–21
 - 21 **Lyshchik A, Higashi T, Asato R et al.** Thyroid gland tumor diagnosis at US elastography. *Radiology* 2005; **237**: 202–11
 - 22 **Itoh A, Ueno E, Tohno E et al.** Breast disease: clinical application of US elastography for diagnosis. *Radiology* 2006; **239**: 341–50
 - 23 **Cochlin DL, Ganatra RH, Griffiths DF.** Elastography in the detection of prostatic cancer. *Clin Radiol* 2002; **57**: 1014–20
 - 24 **Sperandeo G, Sperandeo M, Morcaldi M, Caturelli E, Dimitri L, Camagna A.** Transrectal ultrasonography for the early diagnosis of adenocarcinoma of the prostate: a new maneuver designed to improve the differentiation of malignant and benign lesions. *J Urol* 2003; **169**: 607–10
 - 25 **Halpern EJ.** Contrast-enhanced ultrasound imaging of prostate cancer. *Rev Urol* 2006; **8** (Suppl. 1): S29–37

Correspondence: Leo Pallwein, Department of Radiology 2/Uroradiology, Medical University Innsbruck, Anichstrasse 35, A-6020 Innsbruck, Austria.
e-mail: leo.pallwein@i-med.ac.at

Abbreviations: **US**, ultrasonography, **RTE**, real-time elastography; **RP**, radical prostatectomy; **TZ**, transition zone.